Biophysical Chemistry 335 (2026) 107642

Contents lists available at ScienceDirect

Biophysical Chemistry

journal homepage: www.elsevier.com/locate/biophyschem

An islet amyloid polypeptide oligomer model inhibits fibril formation☆

Anne Pfitzer[a,1], Celina M. Schulz[a,1], Robin Backer[a], Filip Hasecke[a], Lothar Gremer[a,b], Wolfgang Hoyer[a,b,*]

[a] Institut für Physikalische Biologie, Faculty of Mathematics and Natural Sciences, Heinrich Heine University Düsseldorf, Düsseldorf 40204, Germany
[b] Institute of Biological Information Processing (IBI-7: Structural Biochemistry), Forschungszentrum Jülich, Jülich 52428, Germany

ARTICLE INFO

Keywords:
Protein aggregation
Amyloid
IAPP
Amylin
Off-pathway oligomers
Diabetes
Protein engineering

ABSTRACT

Type 2 *diabetes mellitus* (T2DM) is a multifactorial metabolic and widespread disease. In patients' pancreas, islet amyloid polypeptide (IAPP) is found as aggregates. As for other disease-related amyloidogenic proteins, oligomeric species of IAPP have been suggested to exhibit cytotoxic activity. Here, we developed an IAPP model, denoted dimIAPP, which assembles into curvilinear oligomers that persist over extended periods of time. DimIAPP is an engineered dimer of a cysteine-free IAPP mutant (C2S, C7S), with the two dimer subunits linked by a flexible $(G_4S)_4$ linker on one polypeptide chain. In contrast to IAPP, dimIAPP did not form Thioflavin T-positive amyloid fibrils, but assembled into oligomers (dimIAPP-O) which tended to coalesce into larger clusters. IAPP fibril formation was slowed down by addition of dimIAPP-O, a finding that extends previous studies demonstrating an intrinsic inhibitory activity of off-pathway oligomers on amyloid fibril formation. Exposure of pancreatic RIN-m5f cells to dimIAPP-O and IAPP fibrils differentially activated cellular stress response. We conclude that the dimIAPP model is a useful tool to gain further insights into IAPP aggregation and to characterize the effects of off-pathway oligomers of amyloidogenic proteins.

1. Introduction

Loss of β-cell function in T2DM is caused by a multitude of insults. Islet amyloid was found in the pancreatic parenchyma of more than 90% of T2DM patients and is believed to inflict cytotoxicity [1–8]. The main constituent of islet amyloid is IAPP, a 37-residue long peptide hormone co-secreted with insulin [9]. It plays a role in gastric emptying [10], glucose homeostasis [11], regulating satiety [12] and suppression of glucagon release [13]. Amyloid deposits are found in a plethora of diseases, including T2DM, Alzheimer's disease and Parkinson's disease. The unifying feature of these peptides is the characteristic cross-β structure adopted by their amyloid aggregates [14–16]. In T2DM, prominent hyaline lesions were first described in 1901, more than 120 years ago [17,18], in the pancreas of a young patient suffering from hyperglycemia and was later identified as amyloid depositions of IAPP [19,20].

Oligomeric IAPP species have gained increased attention as they might be important players in the pathogenic processes [5–8,21–28]. In support of this, a poor correlation of IAPP amyloid load with β-cell death was observed [29]. Different natural and synthetic IAPP oligomer preparations were characterized and found to exhibit variable levels of toxicity, e.g. to induce apoptosis [30] or disrupt the cell membrane [31]. The exact linkage between IAPP oligomer formation and toxicity is unknown. It has been suggested that IAPP oligomers are related to the formation of a membrane channel inducing an upregulated Ca^{2+} influx or membrane disruption causing stress of the endoplasmic reticulum (ER) [31,32]. However, oligomers are difficult to study, due to their transient nature [33], low population under standard conditions, and structural heterogeneity [34]. This complicates the identification of the most critical species in amyloid diseases [35,36]. It also leads to an uncertainty regarding the position of different types of oligomers on or off the pathway towards amyloid fibrils [34,37–39]. Therefore, it is crucial to invent reliable models for studying oligomers.

Studies on oligomers are not only of great interest in T2DM, but also in over 50 other diseases [40] associated with the assembly of amyloids, like Alzheimer's disease [41–43]. For Alzheimer's amyloid-β (Aβ) it was shown that low-molecular weight species are more toxic than monomers

☆ This article is part of a Special issue entitled: 'condensation/aggregation' published in Biophysical Chemistry.

* Corresponding author at: Institut für Physikalische Biologie, Faculty of Mathematics and Natural Sciences, Heinrich Heine University Düsseldorf, Düsseldorf 40204, Germany.
E-mail address: wolfgang.hoyer@hhu.de (W. Hoyer).

[1] These authors contributed equally: Anne Pfitzer, Celina M. Schulz

https://doi.org/10.1016/j.bpc.2026.107642
Received 31 October 2025; Received in revised form 27 April 2026; Accepted 28 April 2026
Available online 29 April 2026

and fibrils [44]. Previously, we invented a model for oligomer-forming Aβ40, called dimAβ [45–47]. DimAβ is a polypeptide containing two units of Aβ40 connected by a flexible glycine-serine linker. The linkage of two Aβ units does not affect Aβ conformation, but results in an increased local concentration which promotes the highly concentration-dependent oligomer formation. DimAβ assembles into stable curvilinear oligomers that faithfully reflect the properties of off-pathway Aβ oligomers previously observed in many labs, including the binding to dendritic spines and induction of Tau missorting, a key factor in tauopathies [46,48]. DimAβ oligomers provided insight into the properties of off-pathway Aβ oligomers and their relationship to amyloid fibrils [45–47]. For example, metastable dimAβ oligomers bind to the surface of Aβ fibrils and inhibit secondary nucleation [47]. Furthermore, studies employing dimAβ allowed to identify the importance of low pH, as present in endosomal/lysosomal compartments, for rapid Aβ oligomer formation [46].

As stable IAPP oligomers cannot be obtained directly from monomeric human IAPP, the generation of IAPP oligomer models is of great interest. In this study, we tested if oligomers can be obtained using an IAPP construct analogous to dimAβ. This approach is particularly promising due to the sequence similarity of IAPP and Aβ [49,50]. Moreover, certain Aβ and IAPP oligomers may be structurally and functionally related, as suggested by the cross-reactivity of oligomer-specific antibodies [27]. Here, we introduce an engineered IAPP dimer called dimIAPP, characterize the oligomeric species formed by dimIAPP, and report the effect of dimIAPP oligomers on IAPP fibril formation.

2. Results

2.1. DimIAPP assembles into curvilinear oligomers

We developed an artificial IAPP dimer called dimIAPP (Fig. 1), in analogy to the design of the artificial Aβ dimer dimAβ [45]. In dimIAPP, two IAPP units are connected by a $(G_4S)_4$ linker. In the dimAβ construct, this linker did not affect the conformational properties of the Aβ40 subunits and provided sufficient flexibility for the formation of oligomers and amyloid fibrils [45]. We therefore hypothesize that by analogy the identical linker, within dimIAPP, does not restrict the formation of natural IAPP intermediate conformations, oligomers, and amyloid fibrils, including previously described intermediates containing β-sheets, β-hairpin dimers, or α-helices [51–56]. In fully extended conformation, the 20 amino acid linker extends over a length of ~7 nm. This exceeds the distance between the C-terminus of one IAPP subunit and the N-terminus of a second IAPP subunit in structures and structural models of IAPP dimers and oligomers: In the crystal structure of IAPP-maltose binding protein fusions an α-helical IAPP dimer interfaces was established, with a distance between the N-terminus of one subunit and the last resolved residue towards the C-terminus (Ser29) of the other subunit of 2.6 nm [55]. Structural models of IAPP dimers/oligomers comprising both α-helical and β-strand interfaces have been reported both of compact [52] and extended [56] type, with the latter exhibiting distances between the C-terminus of one IAPP subunit and the N-terminus of a second IAPP subunit of up to ~5 nm. The $(G_4S)_4$ linker should thus be compatible with all these IAPP dimer conformations.

In order to avoid formation of aberrant disulfide bonds, the cysteines at positions 2 and 7 of both IAPP units were exchanged to serines (Fig. 1). This modification leads to loss of the disulfide loop connecting IAPP residues 2 and 7 under oxidizing conditions. In fibrils, amino acids (aa)1–12 are usually not part of the core but located at the periphery [16,57–59], indicating that the Cys-to-Ser exchanges are not essential for IAPP aggregation (although fibril polymorphs with ordered regions extending further towards the N-terminus have been obtained [59–61]). Kinetics studies showed that loss of the disulfide loop, e.g. by introduction of the Cys-to-Ser exchanges, actually promotes IAPP amyloid fibril formation [62,63]. Furthermore, we note that dimIAPP is not C-terminally amidated.

We compared protein aggregation of IAPP and dimIAPP by employing the amyloid-specific dye Thioflavin T (ThT). At 2 μM protein concentration and a pH of 6.5, initially monomeric IAPP exhibited an increase in ThT fluorescence after a brief lag-time, indicative of the formation of amyloid fibrils containing cross-β structure (Fig. 2). In contrast, dimIAPP did not show increased ThT fluorescence under these conditions over the 27 h time span of the experiment (Fig. 2).

Atomic force microscopy (AFM) of the samples after 27 h of incubation confirmed amyloid fibril formation of IAPP (Fig. 3A and 4A). In contrast, dimIAPP assembled into spherical and curvilinear oligomers (Fig. 3B and 4B,C). These oligomers, which we named dimIAPP-O, are reminiscent of the metastable off-pathway oligomers formed by dimAβ [45–47]. AFM suggested that curvilinear dimIAPP-O are arranged in a beads-on-a-string fashion (Fig. 4C), as observed before for Aβ oligomers [64]. DimIAPP-O exhibited a strong tendency to assemble into large clusters which can be precipitated by centrifugation (Fig. 3B). The same

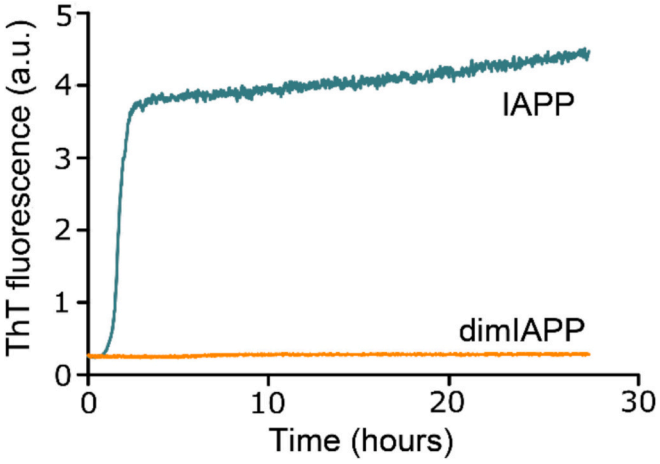

Fig. 2. DimIAPP does not form ThT-positive amyloid aggregates. Aggregation kinetics of IAPP (green) and dimIAPP (orange) monitored by ThT fluorescence. 2 μM of IAPP or dimIAPP were incubated at 37 °C in 50 mM MES, pH 6.5, 50 mM NaCl. (For interpretation of the references to colour in this figure legend, the reader is referred to the web version of this article.)

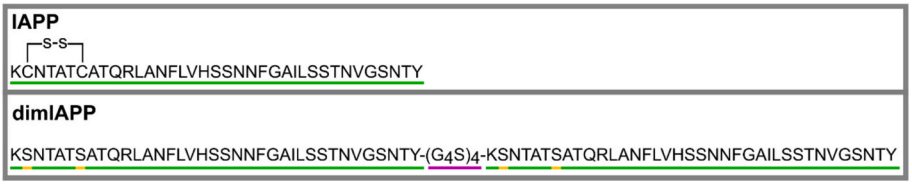

Fig. 1. Model system for IAPP oligomers utilizing a tandem IAPP construct called dimIAPP. Amino acid sequences of IAPP and dimIAPP. DimIAPP incorporates two units of the cysteine-free IAPP mutant IAPP(C2S/C7S) in one polypeptide chain. The subunits are connected via a flexible $(G_4S)_4$ linker (underlined in purple) to provide conformational freedom. Positions of the Cys-to-Ser exchanges are underlined in yellow. (For interpretation of the references to colour in this figure legend, the reader is referred to the web version of this article.)

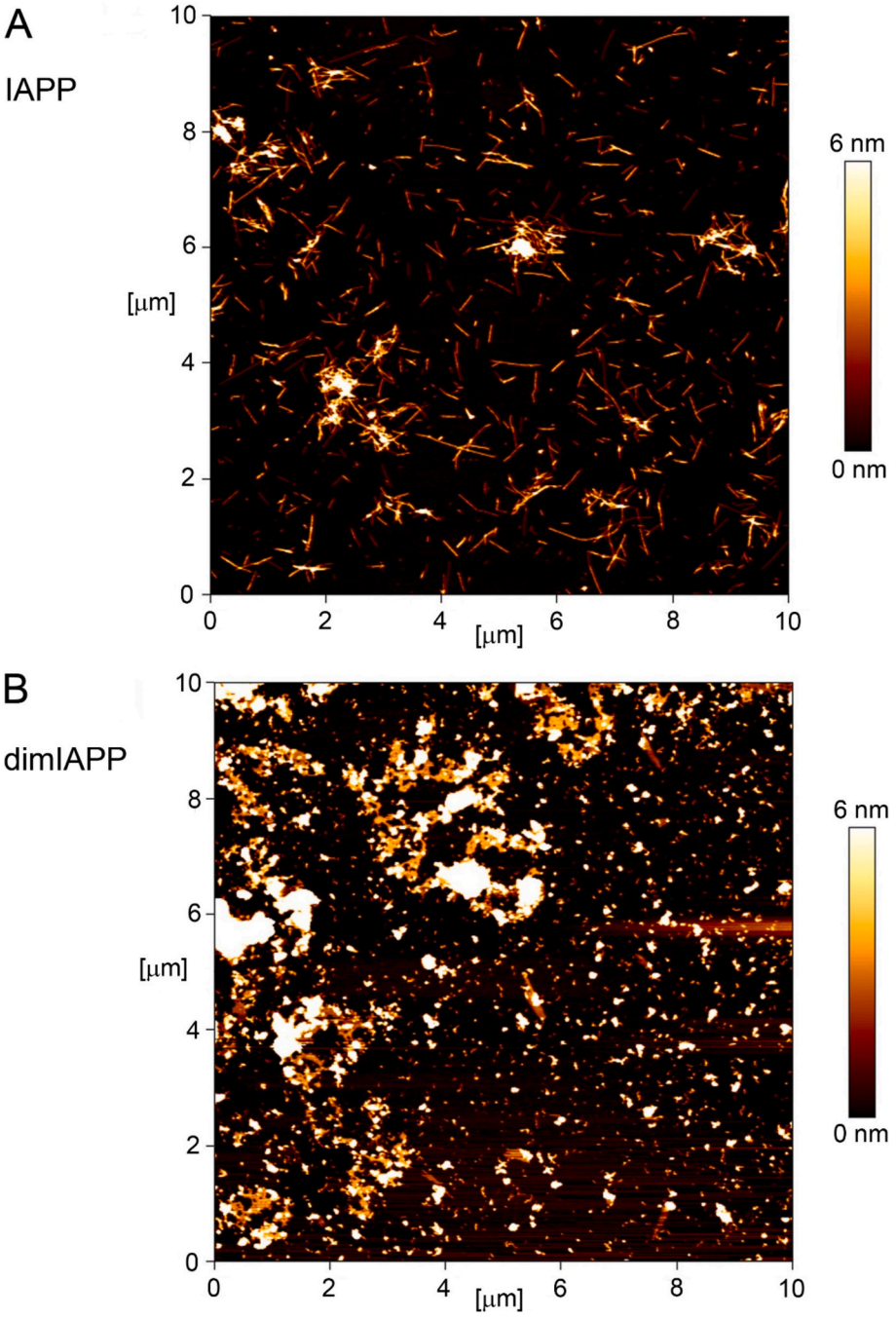

Fig. 3. Aggregate morphologies of IAPP and dimIAPP imaged by AFM. Samples were analyzed after incubation of 2 µM protein samples for 27 h at 37 °C in 50 mM MES, pH 6.5, 50 mM NaCl. Colour scale: height.

has also been observed for dimAβ oligomers at slightly acidic pH [46]. To monitor the kinetics of dimIAPP-O formation, AFM images were taken at different time points (Fig. S1A). Oligomer clusters were visible immediately after preparation of the dimIAPP sample (Fig. S1A), with ~35% of dimIAPP present in the pelletable fraction according to quantification by reversed-phase HPLC (Fig. S1B).

CD spectroscopy was performed to compare the secondary structure of dimIAPP-O to that of IAPP amyloid fibrils (Fig. 5). IAPP amyloid fibrils showed a CD spectrum dominated by β-sheets, with a minimum at 217 nm, in line with the cross-β fibril architecture. In contrast, CD of dimIAPP-O suggested contributions of both α-helical and β-sheet elements, with a broad minimum in the range of 207 to 227 nm.

2.2. *DimIAPP-O inhibit IAPP amyloid fibril formation*

Off-pathway oligomers have been found to exhibit an intrinsic inhibitory activity towards fibril formation [38]. To test if this also applies to dimIAPP-O we investigated the effect of dimIAPP-O on IAPP amyloid fibril formation. DimIAPP-O were formed by pre-incubation of dimIAPP and added at substoichometric ratios to aggregation assays of 3 µM initially monomeric IAPP (Fig. 6). Addition of 0.1 µM dimIAPP-O (all concentrations in dimIAPP monomer units) was sufficient to delay IAPP fibril formation (Fig. 6A). For the tested concentrations of 0.1 µM, 0.25 µM, and 0.5 µM dimIAPP-O, some of the experimental repeats did not show an increase in ThT fluorescence during the 10-h assay, while others exhibited the sigmoidal time course of amyloid fibril formation

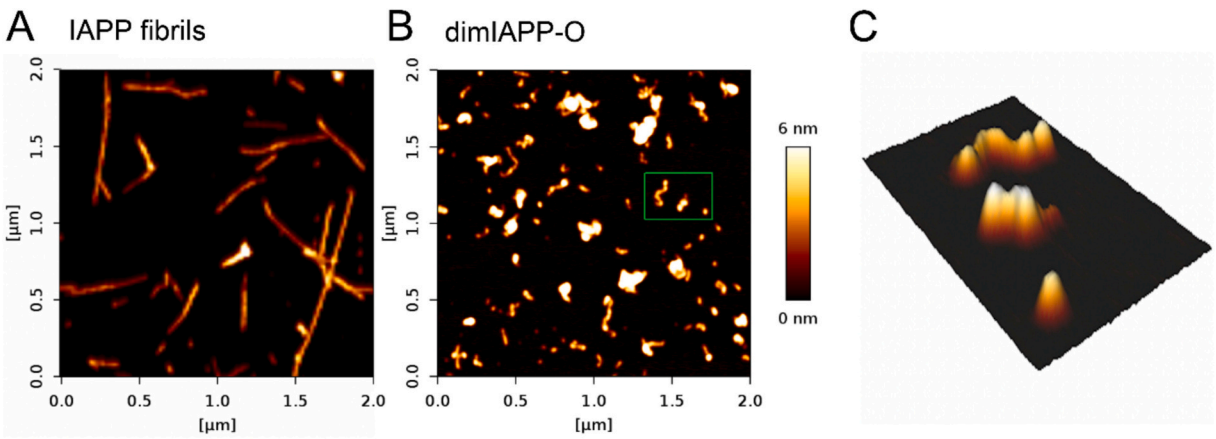

Fig. 4. DimIAPP forms spherical and curvilinear oligomers. AFM images of (A) IAPP fibrils and (B,C) dimIAPP-O. (C) 3D view of spherical and curvilinear dimIAPP-O in a zoomed-in area (marked in green box in B). Colour scale: height. (For interpretation of the references to colour in this figure legend, the reader is referred to the web version of this article.)

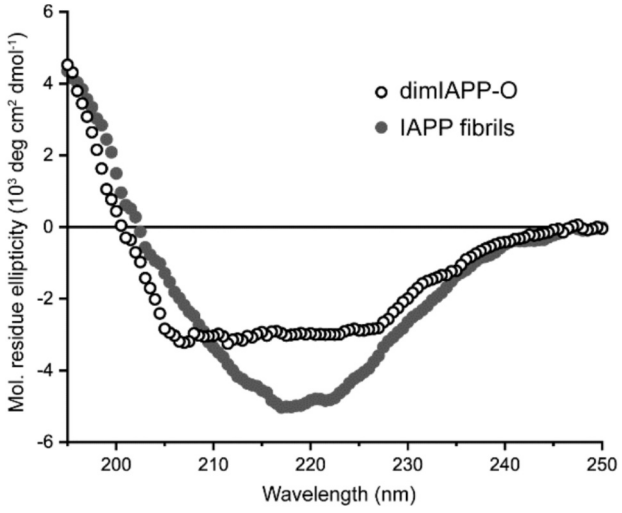

Fig. 5. Secondary structure analysis of dimIAPP-O by far-UV CD spectroscopy. CD spectra of dimIAPP-O and IAPP fibrils recorded at protein concentrations of 5 µM dimIAPP and 10 µM IAPP, respectively.

(Fig. 6A-C). A potential explanation for the heterogeneity of the inhibitory activities might be differences in the extents of supramolecular clustering of dimIAPP-O between samples. Nevertheless, dimIAPP-O showed a clear inhibitory effect at all three concentrations. When ThT did not increase during the assay, AFM did not detect amyloid fibrils but only oligomers at the end of the experiment (Fig. 6D). We conclude that dimIAPP-O efficiently interfere with IAPP amyloid fibril formation.

2.3. Exposure of RIN-m5f cells to dimIAPP-O and IAPP fibrils differentially activates cellular stress response

Oxidative stress and ER stress are believed to play pivotal roles in the pathogenesis of T2DM [65–68]. To gain insights in how the presence of the different aggregation species, IAPP fibrils or dimIAPP-O, affects the induction of stress phenotypes in pancreatic cells, the upregulation of transcripts of stress markers associated with ER stress and mitochondrial oxidative stress was investigated. We were interested exclusively in the effect of externally added IAPP fibrils and dimIAPP-O on stress genes. Therefore, the RIN-m5f cell line derived from *Rattus norvegicus* was selected as model pancreatic cell line because the endogenous rodent IAPP is aggregation-incompetent due to six mutations primarily localized between amino acids 20 and 29. The stress markers *sod2* (superoxide dismutase 2) and *cat* (catalase) were analyzed to investigate oxidative stress [66,68]. Treatment with IAPP fibrils resulted in upregulation of the *cat* gene, while treatment with dimIAPP-O led to an increase in *sod2* transcripts (Fig. 7A,B). Additionally, all tested stress markers for ER stress [65,67], namely *atf6* (activating transcription factor 6), *xbp1* (X-box-binding protein 1), *atf4* (activating transcription factor 4) and *chop* (C/EBP homologous protein) were significantly upregulated after treatment with IAPP fibrils while only *chop*, a key player of apoptosis [69], was upregulated approximately 3-fold after treatment with dimIAPP-O (Fig. 7C-F). These results indicate that IAPP fibrils and dimIAPP-O are stressful to RIN-m5f cells in different ways at the transcriptional level.

3. Discussion

Understanding the mechanisms behind IAPP oligomer toxicity is crucial for developing targeted therapeutic strategies that hold potential for preventing or halting the progression of T2DM [39]. It is of great scientific interest to explore ways to inhibit oligomer formation, promote their clearance, or interfere with their interactions with cell membranes triggering the unfolded protein response (UPR), all in an effort to mitigate the toxic effects of IAPP oligomers and potentially improve diabetes management.

Here, we introduced dimIAPP-O as a stable oligomer model. DimIAPP is constructed in analogy to dimAβ, with the aim to increase the local concentration of the amyloidogenic subunits by direct linkage of two subunits in one polypeptide chain. The increased local concentration supports off-pathway oligomer formation more than it supports fibril formation, due to the higher concentration dependence of off-pathway oligomer formation [45]. In line with the design concept, dimIAPP-O share features with dimAβ-O. They are spherical and curvilinear assemblies a few nm in height (Fig. 4B,C and [45]), with a tendency to coalesce into large clusters (Fig. 3B and [46]). In contrast to dimAβ-O, whose formation kinetics can be monitored by ThT fluorescence [45], dimIAPP-O are ThT-negative. However, this feature does not provide insights into the structural organization of these oligomers, as the molecular basis of ThT binding to oligomers lacking extended cross-β structure is not well understood. It should be noted that dimIAPP-O inevitably differ from native IAPP oligomers in the design of their basic modules, which in the case of dimIAPP-O are dimers of IAPP(C2S/C7S) subunits connected by a flexible, hydrophilic peptide spacer.

DimIAPP-O inhibit IAPP fibril formation (Fig. 5). The same has been previously observed for dimAβ-O and off-pathway oligomers of other amyloidogenic proteins, including α-synuclein, β2-microglobulin, lysozyme, immunoglobulin light chains, and Sup35 [38,45,47,70–76], and

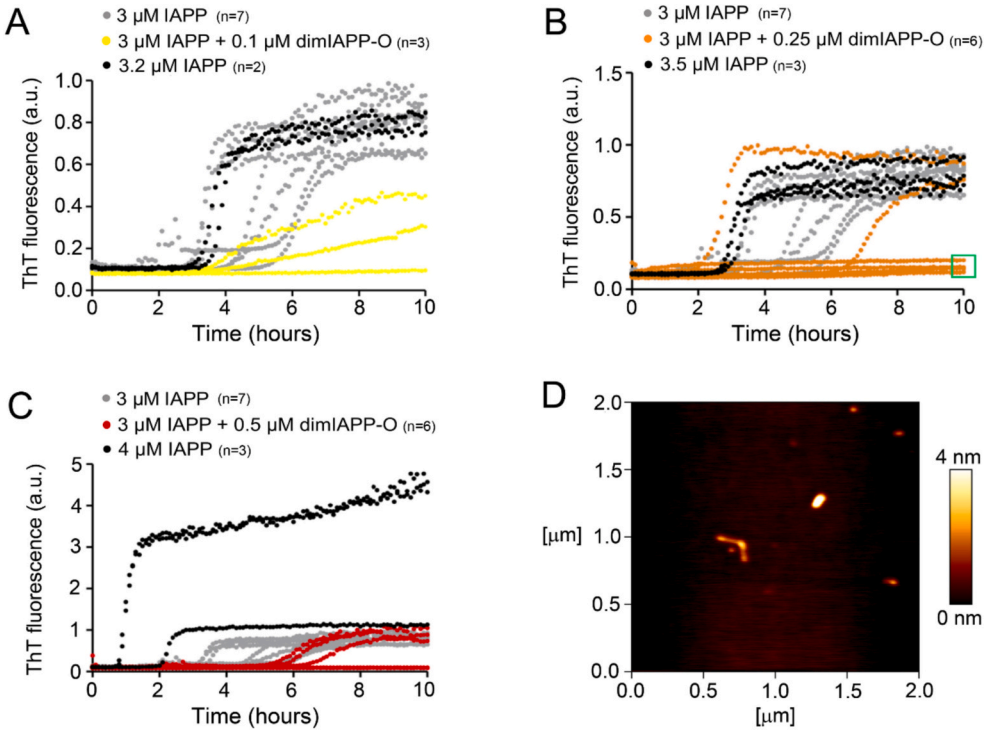

Fig. 6. DimIAPP-O inhibit IAPP fibril formation. (A-C) Time courses of amyloid formation of 3 μM IAPP in the absence (grey) and presence of 0.1 μM dimIAPP-O (A, yellow), 0.25 μM dimIAPP-O (B, orange), or 0.5 μM dimIAPP-O (C, red), in 50 mM MES, pH 6.5, 25 mM $MgCl_2$. For additional comparison, samples containing IAPP at a concentration corresponding to the total IAPP subunit concentration in the +dimIAPP-O samples are given in black. The number of experimental repeats is given in brackets. The same arbitrary scaling factor was applied to all measured fluorescence intensities of all experiments. (D) AFM image taken at the end of incubation of a sample that did not exhibit an increase in ThT fluorescence during the 10-h experiment (marked in green box in B). Colour scale: height. (For interpretation of the references to colour in this figure legend, the reader is referred to the web version of this article.)

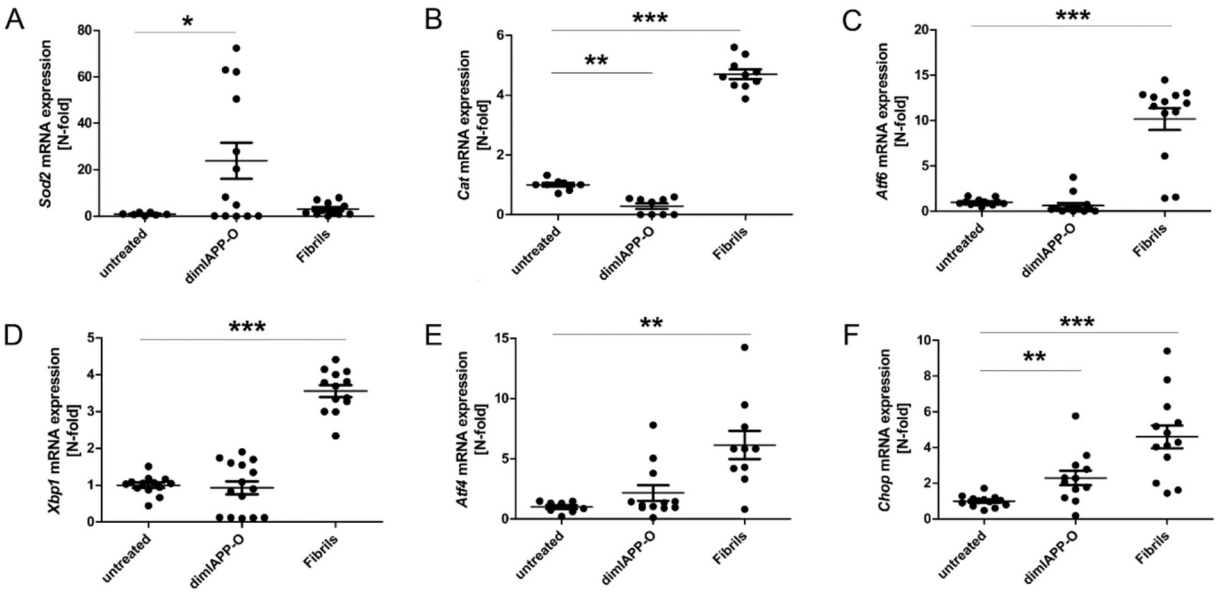

Fig. 7. Effects of dimIAPP-O and IAPP fibrils on transcription of different oxidative stress and ER stress markers. Gene transcription in pancreatic RIN-m5f cells was investigated by qPCR, without or with exposure of the cells to dimIAPP-O or IAPP fibrils at a concentration of 1 μM. (A,B) Oxidative stress markers *sod2* (A) and *cat* (B). (C-E) ER stress markers *atf6* (C), *xbp1* (D), *atf4* (E), and *chop* (F). qPCR analysis was performed in 5 technical replicates and 3 biological replicates. Statistical analysis was applied using an unpaired Student's *t*-test and a Grubb's outlier analysis. * = $p < 0.05$, ** = $p < 0.01$, *** = $p < 0.001$.

therefore qualifies as an intrinsic property of amyloid-forming systems. Mechanistically, inhibition of secondary nucleation processes as a consequence of oligomer-fibril interactions has been shown to contribute to the delay of fibril formation [47,70]. Such a mechanism is in line with the potent inhibition of IAPP fibril formation at substoichiometric concentrations of dimIAPP-O (Fig. 5). Interestingly, previously designed IAPP mimics that inhibited IAPP amyloid formation were found to also assemble into nonfibrillar, albeit soluble, oligomers [77,78].

DimAβ exhibits biphasic aggregation kinetics, with the second phase

representing the formation of amyloid fibrils which slowly replace the initially formed oligomers [45]. This second phase is not observed here for dimIAPP. We propose that kinetic reasons account for the absence of fibril formation. Also in the case of dimAβ, the fibril formation phase is delayed due to increased competition by off-pathway oligomers and only observed under conditions where the nucleation-polymerization mechanism of fibril formation is kinetically accessible, such as in the presence of an air-water interface and mechanical movement in a microtiter plate reader [46]. Similarly, rapid formation of dimIAPP-O might outcompete dimIAPP fibril formation, delaying its observability for a time window beyond the experimental time scale. However, the present data does not rule out that thermodynamic factors might contribute as well. For example, the $(G_4S)_4$ linker might obstruct amyloid fibril formation. This is not expected, as the same linker did not affect the conformational properties when inserted into dimAβ, but it cannot be excluded for the dimIAPP case.

The analysis of stress marker transcription indicates that external addition of dimIAPP-O and IAPP fibrils differentially induces ER stress and oxidative stress responses (Fig. 7). This may be associated with long-term toxicity in a system where progressing protein aggregation triggers disease. However, the physiological relevance of off-pathway IAPP oligomers remains to be elucidated.

We conclude that the dimIAPP-O model provides an attractive path towards the study of off-pathway IAPP oligomers.

4. Materials & methods

4.1. Protein preparation

The dimIAPP expression cassette in the expression vector pET11-a was purchased from Genscript. The expression cassette consists of a 6xHis-tag, one subunit of the IAPP-binding protein β-wrapin HI18, a $(G_4S)_3$ flexible linker, another subunit of the β-wrapin HI18, a $(G_4S)_3$ flexible linker, a TEV cleavage site, the IAPP(C2S/C7S) sequence, a $(G_4S)_4$ flexible linker, and again the IAPP(C2S/C7S) sequence. This design is inspired by the method for recombinant IAPP expression by Mirecka et al. [79]. *E.coli* BL21(DE3) cells were transformed by thawing 200 µl of the cells for 10 min on ice, adding 10 ng of the plasmid, letting cells rest for 10 min on ice, heat shock at 42 °C for 1 min, letting cells rest for 2 min on ice, adding 450 µl of 2YT-medium prewarmed to 37 °C, and letting the cells incubate for 1 h at 37 °C under constant agitation at 800 rpm. Afterwards, the cells were plated on LB agar plates containing ampicillin and incubated at 37 °C overnight.

A preculture was prepared in a volume of 50 ml. The next day, 2 l of main culture were inoculated to an OD_{600} of 0.1, followed by incubation at 37 °C at constant agitation of 120 rpm until an OD_{600} of 0.6 was reached. Expression was performed for 3 h at 37 °C and 120 rpm agitation. Harvesting was performed by centrifugation for 10 min at 5000 xg at 4 °C.

The pellet was dissolved in 10 ml NaPi pH 8, 500 mM NaCl, 6 M Urea and 0.4 mM PMSF. The cells were disrupted with a cell disruptor and spun down for 30 min at 40,000 xg at 4 °C. An IMAC purification was performed in 20 mM NaPi pH 8, 500 mM NaCl, 6 M Urea, including a wash step with 20 mM NaPi pH 8, 500 mM NaCl, 6 M Urea plus 20 mM imidazole. The elution was performed with 20 mM NaPi pH 8, 500 mM NaCl, 6 M Urea plus 450 mM imidazole. The sample was concentrated to 500 µl using a concentrator with 3 MWCO. Size-exclusion chromatography (SEC) was performed using a Superdex200 10/300 Increase column by Cytiva with 20 mM Tris pH 8, 50 mM NaCl as running buffer on an NGC liquid chromatography system (Bio-Rad). The free N-terminus of dimIAPP was obtained by TEV cleavage overnight. Finally, dimIAPP was purified by HPLC on a Zorbax C8 SB300 5 µm 9.4 × 250 mm semipreparative column, using a gradient over 40 min from 20 to 64% AcN, 0.1% TFA. The purity of dimIAPP was 86.5% according to HPLC (Fig. S1C).

IAPP (human) was purchased from Pepscan (purity 93.2%) and aliquoted using 1,1,1,3,3,3-hexfluoro-2-propanol (HFIP). 1 mg IAPP was dissolved in 500 µl of 6 M guanidine hydrochloride. Subsequently, SEC was performed using a Supedex75 10/300 Increase column in 10 mM 2-(N-morpholino) ethanesulfonic acid (MES)/NaOH buffer, pH 6, using a NGC liquid chromatography system (Bio-Rad), and IAPP monomer (purity 93.8%) was collected in Eppendorf Protein LoBind Tubes.

4.2. DimIAPP oligomer (dimIAPP-O) preparation

DimIAPP was aliquoted in 1 µg aliquots using HFIP. One or two aliquots were dissolved in 4 µl of 50 mM NaOH. Then, 92 µl 50 mM MES pH 6.5, 50 mM NaCl were added. Finally, 4 µl 50 mM HCl were added, resulting in 1–2 µM dimIAPP solutions.

To prepare dimIAPP-O for the inhibition tests and CD spectroscopy, the dissolved dimIAPP was quiescently incubated at 37 °C for 16 h. Then, dimIAPP-O were harvested by precipitation at 11,000 xg and 20 °C for 10 min, and the supernatant was discarded. The oligomers were dissolved in buffer at a concentration of 20 µM and then diluted to the desired final concentration.

4.3. IAPP fibril preparation

IAPP was dissolved in 50 mM MES pH 6.5, 50 mM NaCl in a concentration of 100 µM in 50 mM MES pH 6.5, 50 mM NaCl and incubated under constant agitation at 800 rpm for 5 days.

4.4. Thioflavin T (ThT)-fluorescence assays

Aggregation kinetics were monitored by ThT fluorescence in 96-well Half Area Black/Clear Flat Bottom Polystyrene NBS Microplate (Corning, #3881), in the presence of 0.04% NaN_3 and 20 µM ThT. For the inhibition experiments, respective concentrations of pre-formed dimIAPP-O were added to the samples. To allow for comparison with our previous study on inhibition of IAPP aggregation [80], 50 mM MES pH 6.5, 25 mM $MgCl_2$, was used as buffer system. ThT measurements were recorded in a BMG FLUOstar Omega microplate reader with BMG Reader Control software at 37 °C using excitation wavelengths of 448–10 nm and emission wavelengths of 482–10 nm. Each data point reflects to the average of orbitally measured values over 3 mm with 20 flashes per well. The plate was briefly shaken (5 s) at 300 rpm before each measurement cycle.

4.5. AFM imaging

For AFM imaging after ThT kinetics, the plates (96-well Half Area Black/Clear Flat Bottom Polystyrene NBS Microplate, 3881, Corning) were put into a sonication bath for 10 s. Subsequently, 10 µl of the samples were taken out of the plate and put onto a freshly cleaned muscovite mica surface and dried by incubating for 2 min. The mica was washed 3 times with Milli-Q H_2O and blown dry with a steam of N_2. Imaging was done in intermittent contact mode (AC mode) using a JPK NanoWizard 3 AFM with NanoWizard Control Software v.5 version 5.0.84. The cantilever had a silicon tip (OMCL-AC160TS-R3, Olympus) with a tip radius of 9 ± 2 nm, a force constant of 26 N/m and a resonance frequency of 300 kHz.

4.6. CD spectroscopy

Far-UV CD spectra were measured on a JASCO J-815 spectropolarimeter at concentrations of 5 µM dimIAPP and 10 µM IAPP,

respectively, in 1 mm quarz cuvettes (Hellma) at 20 °C.

4.7. HPLC analysis

HPLC analysis was performed on an Agilent 1260 Infinity system using an Agilent Zorbax SB300 C8, 5 µm, 4.6 × 250 mm column at 80 °C column temperature. A flow rate of 0.1 ml/min was applied. After the gradient, the column was washed for 2 min with 80% acetonitrile with 0.1% TFA. Re-equilibration was performed for 8 min using water.

4.8. Cultivation of RIN-m5f cells

RIN-m5f cells (ATCC, CRL-11605, Manassas, VA, USA) were cultured in RPMI-1640 medium (Thermo Fisher ATCC modification, Germany) supplemented with 10% fetal calf serum (Sigma, F9665) and 1% penicillin/streptomycin (ThermoFisher, 15140122) in T75 tissue culture flasks (Sarstedt, 83.3911.002) in a humidified incubator with 5% CO_2 at 37 °C. Depending on their confluence, cells were passaged every three to five days. For the experiments, cells were seeded in well plates (Sarstedt, Cell+ treated). When 80–90% confluence was achieved, cells were treated with IAPP fibrils or dimIAPP-O at a concentration of 1 µM, or with buffer, for 24 h at 37 °C. For RNA isolation, cells were incubated with trypsin for 10 min at 37 °C and then harvested by centrifugation at 5,000 rpm for 5 min. After counting the cells using Neubauer chamber, the cells were dissolved in TRIzol normalized to the same number of cells.

4.9. Quantitative polymerase chain reaction (qPCR)

qPCR was performed using Luna Universal qPCR master mix (New England Biolabs). The 2× master mix was mixed with 0.25 µM of the respective forward and reverse primers. qPCR was performed on a qTOWER3 (Analytik Jena).

CRediT authorship contribution statement

Anne Pfitzer: Writing – original draft, Investigation, Conceptualization. **Celina M. Schulz:** Writing – original draft, Investigation, Conceptualization. **Robin Backer:** Writing – review & editing, Investigation. **Filip Hasecke:** Writing – review & editing, Methodology. **Lothar Gremer:** Investigation. **Wolfgang Hoyer:** Writing – original draft, Supervision, Conceptualization.

Declaration of competing interest

The authors declare that they have no known competing financial interests or personal relationships that could have appeared to influence the work reported in this paper.

Acknowledgements

This project has received funding from the European Research Council under the European Union's Horizon 2020 research and innovation program, grant agreement No. 726368. A.P. thanks the Jürgen Manchot Foundation for funding.

Appendix A. Supplementary data

Supplementary data to this article can be found online at https://doi.org/10.1016/j.bpc.2026.107642.

Data availability

Data will be made available on request.

References

[1] A.E. Butler, J. Janson, S. Bonner-Weir, R. Ritzel, R.A. Rizza, P.C. Butler, β-Cell deficit and increased β-cell apoptosis in humans with type 2 diabetes, Diabetes 52 (2003) 102–110.
[2] S.E. Kahn, S. Andrikopoulos, C.B. Verchere, Islet amyloid: a long-recognized but underappreciated pathological feature of type 2 diabetes, Diabetes 48 (1999) 241–253.
[3] P. Westermark, Amyloid and polypeptide hormones: what is their interrelationship? Amyloid 1 (1994) 47–60.
[4] J. Janson, W.C. Soeller, P.C. Roche, R.T. Nelson, A.J. Torchia, D.K. Kreutter, P. C. Butler, Spontaneous diabetes mellitus in transgenic mice expressing human islet amyloid polypeptide, Proc. Natl. Acad. Sci. USA 93 (1996) 7283–7288.
[5] M.M. Altamirano-Bustamante, N.F. Altamirano-Bustamante, M. Larralde-Laborde, R. Lara-Martínez, E. Leyva-García, E. Garrido-Magaña, G. Rojas, L.F. Jiménez-García, C. Revilla-Monsalve, P. Altamirano, R. Calzada-León, Unpacking the aggregation-oligomerization-fibrillization process of naturally-occurring hIAPP amyloid oligomers isolated directly from sera of children with obesity or diabetes mellitus, Sci. Rep. 9 (2019) 18465.
[6] N.F. Altamirano-Bustamante, E. Garrido-Magaña, E. Morán, A. Calderón, K. Pasten-Hidalgo, R.A. Castillo-Rodríguez, G. Rojas, R. Lara-Martínez, E. Leyva-García, M. Larralde-Laborde, G. Domíguez, C. Murata, Y. Margarita-Vazquez, R. Payro, M. Barbosa, A. Valderrama, H. Montesinos, A. Domínguez-Camacho, V.H. García-Olmos, R. Ferrer, P.G. Medina-Bravo, F. Santoscoy, C. Revilla-Monsalve, L. F. Jiménez-García, J. Morán, J. Villalobos-Alva, M.J. Villalobos, R. Calzada-León, P. Altamirano, M.M. Altamirano-Bustamante, Protein-conformational diseases in childhood: naturally-occurring hIAPP amyloid-oligomers and early β-cell damage in obesity and diabetes, PLoS One 15 (2020) e0237667.
[7] D.C.R. Camargo, D. Garg, K. Buday, A. Franko, A.R. Camargo, F. Schmidt, S.J. Cox, S. Suladze, M. Haslbeck, Y.G. Mideksa, hIAPP forms toxic oligomers in plasma, Chem. Commun. 54 (2018) 5426–5429.
[8] M. Birol, S. Kumar, E. Rhoades, A.D. Miranker, Conformational switching within dynamic oligomers underpins toxic gain-of-function by diabetes-associated amyloid, Nat. Commun. 9 (2018) 1312.
[9] S.E. Kahn, D.A. D'Alessio, M.W. Schwartz, W.Y. Fujimoto, J.W. Ensinck, G. J. Taborsky Jr., D. Porte Jr., Evidence of cosecretion of islet amyloid polypeptide and insulin by beta-cells, Diabetes 39 (1990) 634–638.
[10] H.J. Woerle, M. Albrecht, R. Linke, S. Zschau, C. Neumann, M. Nicolaus, J. E. Gerich, B. Göke, J. Schirra, Impaired hyperglycemia-induced delay in gastric emptying in patients with type 1 diabetes deficient for islet amyloid polypeptide, Diabetes Care 31 (2008) 2325–2331.
[11] A. Kanatsuka, H. Makino, H. Ohsawa, Y. Tokuyama, T. Yamaguchi, S. Yoshida, M. Adachi, Secretion of islet amyloid polypeptide in response to glucose, FEBS Lett. 259 (1989) 199–201.
[12] U. Arnelo, M.K. Herrington, E. Theodorsson, T.E. Adrian, R. Reidelberger, J. Larsson, J. Marcusson, L. Strommer, X. Ding, J. Permert, Effects of long-term infusion of anorexic concentrations of islet amyloid polypeptide on neurotransmitters and neuropeptides in rat brain, Brain Res. 887 (2000) 391–398.
[13] B. Åkesson, G. Panagiotidis, P. Westermark, I. Lundquist, Islet amyloid polypeptide inhibits glucagon release and exerts a dual action on insulin release from isolated islets, Regul. Pept. 111 (2003) 55–60.
[14] L. Gremer, D. Schölzel, C. Schenk, E. Reinartz, J. Labahn, R.B. Ravelli, M. Tusche, C. Lopez-Iglesias, W. Hoyer, H. Heise, Fibril structure of amyloid-β (1–42) by cryo–electron microscopy, Science 358 (2017) 116–119.
[15] R. Guerrero-Ferreira, N.M. Taylor, D. Mona, P. Ringler, M.E. Lauer, R. Riek, M. Britschgi, H. Stahlberg, Cryo-EM structure of alpha-synuclein fibrils, eLife 7 (2018) e36402.
[16] C. Roeder, T. Kupreichyk, L. Gremer, L.U. Schäfer, K.R. Pothula, R.B. Ravelli, D. Willbold, W. Hoyer, G.F. Schröder, Cryo-EM structure of islet amyloid polypeptide fibrils reveals similarities with amyloid-β fibrils, Nat. Struct. Mol. Biol. 27 (2020) 660–667.
[17] E.L. Opie, On the relation of chronic interstitial pancreatitis to the islands of Langerhans and to diabetes melutus, J. Exp. Med. 5 (1901) 397–428.
[18] A. Weichselbaum, E. Stangl, Zur Kenntnis der feineren Veränderungen des Pankreas bei Diabetes mellitus, Wien. Klin. Wochenschr. 14 (1901) 968–972.
[19] P. Westermark, C. Wernstedt, E. Wilander, K. Sletten, A novel peptide in the calcitonin gene related peptide family as an amyloid fibril protein in the endocrine pancreas, Biochem. Biophys. Res. Commun. 140 (1986) 827–831.
[20] P. Westermark, C. Wernstedt, E. Wilander, D.W. Hayden, T.D. O'Brien, K. H. Johnson, Amyloid fibrils in human insulinoma and islets of Langerhans of the diabetic cat are derived from a neuropeptide-like protein also present in normal islet cells, Proc. Natl. Acad. Sci. USA 84 (1987) 3881–3885.
[21] A. Abedini, A. Plesner, P. Cao, Z. Ridgway, J. Zhang, L.-H. Tu, C.T. Middleton, B. Chao, D.J. Sartori, F. Meng, Time-resolved studies define the nature of toxic IAPP intermediates, providing insight for anti-amyloidosis therapeutics, Elife 5 (2016) e12977.
[22] L. Haataja, T. Gurlo, C.J. Huang, P.C. Butler, Islet amyloid in type 2 diabetes, and the toxic oligomer hypothesis, Endocr. Rev. 29 (2008) 303–316.
[23] A.E. Butler, J. Janson, W.C. Soeller, P.C. Butler, Increased beta-cell apoptosis prevents adaptive increase in beta-cell mass in mouse model of type 2 diabetes: evidence for role of islet amyloid formation rather than direct action of amyloid, Diabetes 52 (2003) 2304–2314.
[24] T. Gurlo, S. Ryazantsev, C.J. Huang, M.W. Yeh, H.A. Reber, O.J. Hines, T. D. O'Brien, C.G. Glabe, P.C. Butler, Evidence for proteotoxicity in beta cells in type 2 diabetes: toxic islet amyloid polypeptide oligomers form intracellularly in the secretory pathway, Am. J. Pathol. 176 (2010) 861–869.

[25] C.-Y. Lin, T. Gurlo, R. Kayed, A.E. Butler, L. Haataja, C.G. Glabe, P.C. Butler, Toxic human islet amyloid polypeptide (h-IAPP) oligomers are intracellular, and vaccination to induce anti-toxic oligomer antibodies does not prevent h-IAPP–induced β-cell apoptosis in h-IAPP transgenic mice, Diabetes 56 (2007) 1324–1332.
[26] S.L. Masters, A. Dunne, S.L. Subramanian, R.L. Hull, G.M. Tannahill, F.A. Sharp, C. Becker, L. Franchi, E. Yoshihara, Z. Chen, N. Mullooly, L.A. Mielke, J. Harris, R. C. Coll, K.H. Mills, K.H. Mok, P. Newsholme, G. Nuñez, J. Yodoi, S.E. Kahn, E. C. Lavelle, L.A. O'Neill, Activation of the NLRP3 inflammasome by islet amyloid polypeptide provides a mechanism for enhanced IL-1β in type 2 diabetes, Nat. Immunol. 11 (2010) 897–904.
[27] R. Kayed, E. Head, J.L. Thompson, T.M. McIntire, S.C. Milton, C.W. Cotman, C. G. Glabe, Common structure of soluble amyloid oligomers implies common mechanism of pathogenesis, Science 300 (2003) 486–489.
[28] P. Westermark, A. Andersson, G.T. Westermark, Islet amyloid polypeptide, islet amyloid, and diabetes mellitus, Physiol. Rev. 91 (2011) 795–826.
[29] J.J. Meier, R. Kayed, C.-Y. Lin, T. Gurlo, L. Haataja, S. Jayasinghe, R. Langen, C. G. Glabe, P.C. Butler, Inhibition of human IAPP fibril formation does not prevent β-cell death: evidence for distinct actions of oligomers and fibrils of human IAPP, Am. J. Physiol.-Endocrinol. Metabol. 291 (2006) E1317–E1324.
[30] Y. Bram, A. Frydman-Marom, I. Yanai, S. Gilead, R. Shaltiel-Karyo, N. Amdursky, E. Gazit, Apoptosis induced by islet amyloid polypeptide soluble oligomers is neutralized by diabetes-associated specific antibodies, Sci. Rep. 4 (2014) 4267.
[31] J. Janson, R.H. Ashley, D. Harrison, S. McIntyre, P.C. Butler, The mechanism of islet amyloid polypeptide toxicity is membrane disruption by intermediate-sized toxic amyloid particles, Diabetes 48 (1999) 491–498.
[32] M. Kawahara, Y. Kuroda, N. Arispe, E. Rojas, Alzheimer's beta-amyloid, human islet amylin, and prion protein fragment evoke intracellular free calcium elevations by a common mechanism in a hypothalamic GnRH neuronal cell line, J. Biol. Chem. 275 (2000) 14077–14083.
[33] E.E. Cawood, T.K. Karamanos, A.J. Wilson, S.E. Radford, Visualizing and trapping transient oligomers in amyloid assembly pathways, Biophys. Chem. 268 (2021) 106505.
[34] C. Berardet, J. Kaffy, F. Halgand, G. Van der Rest, S. Ongeri, M. Taverna, Evidence for different in vitro oligomerization behaviors of synthetic hIAPP obtained from different sources, Anal. Bioanal. Chem. 412 (2020) 3103–3111.
[35] D.M. Walsh, D.J. Selkoe, Aβ oligomers – a decade of discovery, J. Neurochem. 101 (2007) 1172–1184.
[36] E.N. Cline, M.A. Bicca, K.L. Viola, W.L. Klein, The amyloid-β oligomer hypothesis: beginning of the third decade, J. Alzheimer's Dis 64 (2018) S567–s610.
[37] A.J. Dear, G. Meisl, A. Saric, T.C.T. Michaels, M. Kjaergaard, S. Linse, T.P. J. Knowles, Identification of on- and off-pathway oligomers in amyloid fibril formation, Chem. Sci. 11 (2020) 6236–6247.
[38] M. Muschol, W. Hoyer, Amyloid oligomers as on-pathway precursors or off-pathway competitors of fibrils, Front. Mol. Biosci. 10 (2023) 1120416.
[39] S. Zraika, R.L. Hull, C.B. Verchere, A. Clark, K.J. Potter, P.E. Fraser, D.P. Raleigh, S. E. Kahn, Toxic oligomers and islet beta cell death: guilty by association or convicted by circumstantial evidence? Diabetologia 53 (2010) 1046–1056.
[40] M.G. Iadanza, M.P. Jackson, E.W. Hewitt, N.A. Ranson, S.E. Radford, A new era for understanding amyloid structures and disease, Nat. Rev. Mol. Cell Biol. 19 (2018) 755–773.
[41] J.P. Cleary, D.M. Walsh, J.J. Hofmeister, G.M. Shankar, M.A. Kuskowski, D. J. Selkoe, K.H. Ashe, Natural oligomers of the amyloid-beta protein specifically disrupt cognitive function, Nat. Neurosci. 8 (2005) 79–84.
[42] R. Kayed, Y. Sokolov, B. Edmonds, T.M. McIntire, S.C. Milton, J.E. Hall, C.G. Glabe, Permeabilization of lipid bilayers is a common conformation-dependent activity of soluble amyloid oligomers in protein misfolding diseases, J. Biol. Chem. 279 (2004) 46363–46366.
[43] M.N. Vieira, L. Forny-Germano, L.M. Saraiva, A. Sebollela, A.M. Martinez, J. C. Houzel, F.G. De Felice, S.T. Ferreira, Soluble oligomers from a non-disease related protein mimic Abeta-induced tau hyperphosphorylation and neurodegeneration, J. Neurochem. 103 (2007) 736–748.
[44] K. Ono, M.M. Condron, D.B. Teplow, Structure–neurotoxicity relationships of amyloid β-protein oligomers, Proc. Natl. Acad. Sci. 106 (2009) 14745–14750.
[45] F. Hasecke, T. Miti, C. Perez, J. Barton, D. Schölzel, L. Gremer, C.S. Grüning, G. Matthews, G. Meisl, T.P. Knowles, Origin of metastable oligomers and their effects on amyloid fibril self-assembly, Chem. Sci. 9 (2018) 5937–5948.
[46] M.P. Schützmann, F. Hasecke, S. Bachmann, M. Zielinski, S. Hänsch, G.F. Schröder, H. Zempel, W. Hoyer, Endo-lysosomal aβ concentration and pH trigger formation of aβ oligomers that potently induce tau missorting, Nat. Commun. 12 (2021) 4634.
[47] F. Hasecke, C. Niyangoda, G. Borjas, J. Pan, G. Matthews, M. Muschol, W. Hoyer, Protofibril–fibril interactions inhibit amyloid fibril assembly by obstructing secondary nucleation, Angew. Chem. 133 (2021) 3053–3058.
[48] M. Yuan, X. Tang, W. Han, Anatomy and formation mechanisms of early amyloid-β oligomers with lateral branching: graph network analysis on large-scale simulations, Chem. Sci. 13 (2022) 2649–2660.
[49] E. Andreetto, L.M. Yan, M. Tatarek-Nossol, A. Velkova, R. Frank, A. Kapurniotu, Identification of hot regions of the aβ–IAPP interaction interface as high-affinity binding sites in both cross-and self-association, Angew. Chem. Int. Ed. 49 (2010) 3081–3085.
[50] B. O'Nuallain, A.D. Williams, P. Westermark, R. Wetzel, Seeding specificity in amyloid growth induced by heterologous fibrils, J. Biol. Chem. 279 (2004) 17490–17499.
[51] L.E. Buchanan, E.B. Dunkelberger, H.Q. Tran, P.N. Cheng, C.C. Chiu, P. Cao, D. P. Raleigh, J.J. de Pablo, J.S. Nowick, M.T. Zanni, Mechanism of IAPP amyloid fibril formation involves an intermediate with a transient beta-sheet, Proc. Natl. Acad. Sci. USA 110 (2013) 19285–19290.
[52] N.F. Dupuis, C. Wu, J.E. Shea, M.T. Bowers, The amyloid formation mechanism in human IAPP: dimers have beta-strand monomer-monomer interfaces, J. Am. Chem. Soc. 133 (2011) 7240–7243.
[53] E.A. Mirecka, S. Feuerstein, L. Gremer, G.F. Schroder, M. Stoldt, D. Willbold, W. Hoyer, β-Hairpin of islet amyloid polypeptide bound to an aggregation inhibitor, Sci. Rep. 6 (2016) 33474.
[54] A. Abedini, D.P. Raleigh, A critical assessment of the role of helical intermediates in amyloid formation by natively unfolded proteins and polypeptides, Protein Eng. Des. Sel. 22 (2009) 453–459.
[55] J.J. Wiltzius, S.A. Sievers, M.R. Sawaya, D. Eisenberg, Atomic structures of IAPP (amylin) fusions suggest a mechanism for fibrillation and the role of insulin in the process, Protein Sci. 18 (2009) 1521–1530.
[56] S.T. Shivani, B.E. LeMasters, T. Ravula, H.J. Esterly, N. Maroli, K.L. Rich, C. R. Fields, S.S. Dicke, O.A. Warmuth, D.S. Stapleton, M.P. Keller, A.D. Attie, A. A. Kananenka, K.A. Henzler-Wildman, C.M. Rienstra, M.T. Zanni, A structural model of toxic amyloid oligomers involved in type 2 diabetes, Proc. Natl. Acad. Sci. USA 123 (2026) e2528103123.
[57] R. Gallardo, M.G. Iadanza, Y. Xu, G.R. Heath, R. Foster, S.E. Radford, N.A. Ranson, Fibril structures of diabetes-related amylin variants reveal a basis for surface-templated assembly, Nat. Struct. Mol. Biol. 27 (2020) 1048–1056.
[58] Q. Cao, D.R. Boyer, M.R. Sawaya, P. Ge, D.S. Eisenberg, Cryo-EM structure and inhibitor design of human IAPP (amylin) fibrils, Nat. Struct. Mol. Biol. 27 (2020) 653–659.
[59] Q. Cao, D.R. Boyer, M.R. Sawaya, R. Abskharon, L. Saelices, B.A. Nguyen, J. Lu, K. A. Murray, F. Kandeel, D.S. Eisenberg, Cryo-EM structures of hIAPP fibrils seeded by patient-extracted fibrils reveal new polymorphs and conserved fibril cores, Nat. Struct. Mol. Biol. 28 (2021) 724–730.
[60] D. Li, X. Zhang, Y. Wang, H. Zhang, K. Song, K. Bao, P. Zhu, A new polymorphism of human amylin fibrils with similar protofilaments and a conserved core, iScience 25 (2022) 105705.
[61] S.A. Ooi, D. Valli, M.I. Kuska, H. Mari, H. Chaudhary, W.Y. Wahlgren, S. Westenhoff, A.A. Tietze, A. Novials, J.M. Servitja, M. Maj, Cryo-EM exposes diverse polymorphism in IAPP mutants to guide the rational design of peptide-based therapeutics, J. Mol. Biol. 437 (2025) 169405.
[62] B.W. Koo, A.D. Miranker, Contribution of the intrinsic disulfide to the assembly mechanism of islet amyloid, Protein Sci. 14 (2005) 231–239.
[63] Z. Ridgway, X. Zhang, A.G. Wong, A. Abedini, A.M. Schmidt, D.P. Raleigh, Analysis of the role of the conserved disulfide in amyloid formation by human islet amyloid polypeptide in homogeneous and heterogeneous environments, Biochemistry 57 (2018) 3065–3074.
[64] B.A. Chromy, R.J. Nowak, M.P. Lambert, K.L. Viola, L. Chang, P.T. Velasco, B. W. Jones, S.J. Fernandez, P.N. Lacor, P. Horowitz, C.E. Finch, G.A. Krafft, W. L. Klein, Self-assembly of Abeta(1-42) into globular neurotoxins, Biochemistry 42 (2003) 12749–12760.
[65] S.H. Back, R.J. Kaufman, Endoplasmic reticulum stress and type 2 diabetes, Annu. Rev. Biochem. 81 (2012) 767–793.
[66] E. Cecerska-Heryc, W. Engwert, J. Michalow, J. Marciniak, R. Birger, N. Serwin, R. Heryc, A. Polikowska, M. Goszka, B. Wojciuk, M. Wisniewska, B. Dolegowska, Oxidative stress markers and inflammation in type 1 and 2 diabetes are affected by BMI, treatment type, and complications, Sci. Rep. 15 (2025) 23605.
[67] Z. He, Q. Liu, Y. Wang, B. Zhao, L. Zhang, X. Yang, Z. Wang, The role of endoplasmic reticulum stress in type 2 diabetes mellitus mechanisms and impact on islet function, PeerJ 13 (2025) e19192.
[68] A. Caturano, M. D'Angelo, A. Mormone, V. Russo, M.P. Mollica, T. Salvatore, R. Galiero, L. Rinaldi, E. Vetrano, R. Marfella, M. Monda, A. Giordano, F.C. Sasso, Oxidative stress in type 2 diabetes: impacts from pathogenesis to lifestyle modifications, Curr. Issues Mol. Biol. 45 (2023) 6651–6666.
[69] Y. Li, Y. Guo, J. Tang, J. Jiang, Z. Chen, New insights into the roles of CHOP-induced apoptosis in ER stress, Acta Biochim. Biophys. Sin. Shanghai 46 (2014) 629–640.
[70] M.P. Schützmann, W. Hoyer, Off-pathway oligomers of α-synuclein and aβ inhibit secondary nucleation of α-synuclein amyloid fibrils, J. Mol. Biol. 437 (2025) 169048.
[71] T.R. Serio, A.G. Cashikar, A.S. Kowal, G.J. Sawicki, J.J. Moslehi, L. Serpell, M. F. Arnsdorf, S.L. Lindquist, Nucleated conformational conversion and the replication of conformational information by a prion determinant, Science 289 (2000) 1317–1321.
[72] P.O. Souillac, V.N. Uversky, I.S. Millett, R. Khurana, S. Doniach, A.L. Fink, Elucidation of the molecular mechanism during the early events in immunoglobulin light chain amyloid fibrillation. evidence for an off-pathway oligomer at acidic pH, J. Biol. Chem. 277 (2002) 12666–12679.
[73] W.S. Gosal, I.J. Morten, E.W. Hewitt, D.A. Smith, N.H. Thomson, S.E. Radford, Competing pathways determine fibril morphology in the self-assembly of beta2-microglobulin into amyloid, J. Mol. Biol. 351 (2005) 850–864.
[74] S.E. Hill, T. Miti, T. Richmond, M. Muschol, Spatial extent of charge repulsion regulates assembly pathways for lysozyme amyloid fibrils, PLoS One 6 (2011) e18171.
[75] J. Foley, S.E. Hill, T. Miti, M. Mulaj, M. Ciesla, R. Robeel, C. Persichilli, R. Raynes, S. Westerheide, M. Muschol, Structural fingerprints and their evolution during oligomeric vs. oligomer-free amyloid fibril growth, J. Chem. Phys. 139 (2013) 121901.
[76] T. Miti, M. Mulaj, J.D. Schmit, M. Muschol, Stable, metastable, and kinetically trapped amyloid aggregate phases, Biomacromolecules 16 (2015) 326–335.

[77] L.M. Yan, M. Tatarek-Nossol, A. Velkova, A. Kazantzis, A. Kapurniotu, Design of a mimic of nonamyloidogenic and bioactive human islet amyloid polypeptide (IAPP) as nanomolar affinity inhibitor of IAPP cytotoxic fibrillogenesis, Proc. Natl. Acad. Sci. USA 103 (2006) 2046–2051.

[78] L.M. Yan, A. Velkova, M. Tatarek-Nossol, G. Rammes, A. Sibaev, E. Andreetto, M. Kracklauer, M. Bakou, E. Malideli, B. Goke, J. Schirra, M. Storr, A. Kapurniotu, Selectively N-methylated soluble IAPP mimics as potent IAPP receptor agonists and nanomolar inhibitors of cytotoxic self-assembly of both IAPP and Abeta40, Angew. Chem. Int. Ed. Eng. 52 (2013) 10378–10383.

[79] E.A. Mirecka, L. Gremer, S. Schiefer, F. Oesterhelt, M. Stoldt, D. Willbold, W. Hoyer, Engineered aggregation inhibitor fusion for production of highly amyloidogenic human islet amyloid polypeptide, J. Biotechnol. 191 (2014) 221–227.

[80] R. Törner, T. Kupreichyk, L. Gremer, E.C. Debled, D. Fenel, S. Schemmert, P. Gans, D. Willbold, G. Schoehn, W. Hoyer, J. Boisbouvier, Structural basis for the inhibition of IAPP fibril formation by the co-chaperonin prefoldin, Nat. Commun. 13 (2022) 2363.